ResearchGate

See discussions, stats, and author profiles for this publication at: https://www.researchgate.net/publication/248746646

Nucleation and Growth During Al2O3 Atomic Layer Deposition on Polymers

ARTICLE *in* CHEMISTRY OF MATERIALS · NOVEMBER 2005

Impact Factor: 8.35 · DOI: 10.1021/cm050704d

CITATIONS
200

READS
33

3 AUTHORS, INCLUDING:

Robert H. Grubbs
California Institute of Technology
718 PUBLICATIONS **48,780** CITATIONS
SEE PROFILE

S.M. George
University of Colorado at Boulder
183 PUBLICATIONS **8,164** CITATIONS
SEE PROFILE

Available from: Robert H. Grubbs
Retrieved on: 16 January 2016

Nucleation and Growth during Al_2O_3 Atomic Layer Deposition on Polymers

C. A. Wilson,† R. K. Grubbs,† and S. M. George,*,†,‡

Departments of Chemistry and Biochemistry and Chemical and Biological Engineering, University of Colorado, Boulder, Colorado 80309-0215

Received April 1, 2005. Revised Manuscript Received August 29, 2005

Nucleation and growth during Al_2O_3 atomic layer deposition (ALD) were explored on a variety of polymer films at 85 °C. Al_2O_3 ALD was performed using sequential exposures of $Al(CH_3)_3$ [trimethylaluminum (TMA)] and H_2O. The polymer films were polystyrene (PS), polypropylene (PP), poly(methyl methacrylate) (PMMA), polyethylene (PE), and poly(vinyl chloride) (PVC). These polymer films were prepared by spin-coating onto the surface of a quartz crystal microbalance (QCM) sensor or the surface of a Si(100) wafer. Al_2O_3 ALD during the sequential TMA and H_2O exposures was monitored in situ on the various polymers using the QCM. The QCM measurements revealed distinct differences for each polymer in the initial nucleation period during Al_2O_3 ALD. Following the initial nucleation period, linear Al_2O_3 ALD growth was observed on all the polymers. The thickness of the Al_2O_3 ALD films was also characterized by ex situ surface profilometry. Based on the QCM measurements and recent FTIR measurements of Al_2O_3 ALD on low-density PE, a model is proposed for Al_2O_3 ALD nucleation and growth on polymers. This model is based on the adsorption of TMA onto the surface and absorption into the near-surface region of the polymer. The adsorbed and absorbed TMA is then available for subsequent reaction with the H_2O exposure. This model for Al_2O_3 ALD does not require specific chemical groups on the polymer surface to initiate Al_2O_3 ALD. This model should be valuable to understand and optimize the use of these Al_2O_3 ALD films as seed layers and gas diffusion barriers on polymers.

I. Introduction

Atomic layer deposition (ALD) is a thin film growth technique based on sequential self-limiting surface reactions.[1,2] In the typical ALD process for a binary compound, two gas phase molecules are alternatively exposed to a substrate in an ABAB... sequence. The (A) gas exposure reacts with surface species, adds the first desired atomic element, and changes the surface species. The subsequent (B) gas exposure reacts with the new surface groups and adds the second desired atomic element. This second reaction also changes the surface groups back to the original surface species. The ABAB... sequence can deposit thin films conformally with atomic layer control. A variety of binary materials can be grown using a multitude of ALD surface chemistries.[3]

Al_2O_3 ALD using $Al(CH_3)_3$ and H_2O is one of the most studied ALD systems.[4−7] Al_2O_3 ALD can be deposited on thermally sensitive polymers because Al_2O_3 ALD can be conducted at temperatures as low as 35 °C.[6] The ability to coat Al_2O_3 onto polymers provides a pathway to fabricate inorganic−organic composites with novel properties.[8] Al_2O_3 ALD has been demonstrated on low-density polyethylene (PE) polymer particles at 77 °C.[9] An Al_2O_3 ALD adhesion layer on SiLK polymeric low *k* dielectric material was used to facilitate TiN ALD.[10] Al_2O_3 ALD films were used to form gas diffusion barriers on Kapton and polyethylene naphthalene 2,6-dicarboxylate (PEN) polymeric films to prevent H_2O and O_2 permeation.[11] In addition, plasma-enhanced Al_2O_3 ALD has been employed to coat polyethersulfone polymeric substrates.[12] Lifetime improvements of organic light-emitting diodes (OLEDs) also resulted from plasma-enhanced Al_2O_3 ALD films.[13]

Despite the many applications for Al_2O_3 ALD on polymers, there is little understanding of the nucleation and growth of Al_2O_3 ALD on polymers. The absence of chemical groups on the polymer surface initially suggests that the

* To whom correspondence should be addressed.
† Department of Chemistry and Biochemistry.
‡ Department of Chemical and Biological Engineering.

(1) Suntola, T. *Thin Solid Films* **1992**, *216*, 84.
(2) George, S. M.; Ott, A. W.; Klaus, J. W. *J. Phys. Chem.* **1996**, *100*, 13121.
(3) Ritala, M.; Leskela, M. Atomic Layer Deposition. In *Handbook of Thin Film Materials*; Nalwa, H. S., Ed.; Academic Press: San Diego, 2001.
(4) Dillon, A. C.; Ott, A. W.; Way, J. D.; George, S. M. *Surf. Sci.* **1995**, *322*, 230.
(5) Ott, A. W.; Klaus, J. W.; Johnson, J. M.; George, S. M. *Thin Solid Films* **1997**, *292*, 135.
(6) Groner, M. D.; Fabreguette, F. H.; Elam, J. W.; George, S. M. *Chem. Mater.* **2003**, *16*, 639.
(7) Ritala, M.; Leskela, M.; Dekker: J. P.; Mutsaers, C.; Soininen, P. J.; Skarp, J. *Chem. Vap. Dep.* **1999**, *5*, 7.
(8) LeBaron, P. C.; Wang, Z.; Pinnavaia, T. J. *Appl. Clay Sci.* **1999**, *15*, 11.
(9) Ferguson, J. D.; Weimer, A. W.; George, S. M. *Chem. Mater.* **2004**, *16*, 5602.
(10) Elam, J. W.; Wilson, C. A.; Schuisky, M.; Sechrist, Z. A.; George, S. M. *J. Vac. Sci. Technol. B* **2003**, *21*, 1099.
(11) Groner, M. D.; George, S. M. McLean, R. S. Carcia, P. F. Submitted to *Appl. Phys. Lett.* **2005**.
(12) Yun, S. J.; Lim, J. W.; Lee, J. H. *Electrochem. Solid State Lett.* **2004**, *7*, C13.
(13) Yun, S. J.; Ko, Y. W.; Lim, J. W. *Appl. Phys. Lett.* **2004**, *85*, 4896.

10.1021/cm050704d CCC: $30.25 © 2005 American Chemical Society
Published on Web 10/13/2005

nucleation of Al_2O_3 ALD should be very difficult.[9] Calculations have shown that Al_2O_3 ALD easily nucleates and grows on $-OH$ and $-NH_2$ terminated self-assembled monolayers (SAMs).[14] However, there is no thermodynamic driving force for Al_2O_3 ALD on $-CH_3$ terminated SAMs that resemble hydrocarbon polymers.[14] The recent demonstrations of Al_2O_3 ALD on low-density PE, SiLK, Kapton, and PEN argue that alternative nucleation mechanisms may exist that do not require specific chemical groups on the polymer surface.

The nucleation and growth of Al_2O_3 ALD on polymers is especially important for the development of effective gas diffusion barrier layers on organic electronic devices.[15] The most demanding gas diffusion barriers needed for OLEDs require films with an absolute minimum of defects or pinholes and H_2O permeabilities on the order of 1×10^{-6} g/m^2 day.[16] The continuous and pinhole-free characteristics of Al_2O_3 ALD films lead to extremely low electrical leakage through Al_2O_3 ALD films.[17] This behavior suggests that these Al_2O_3 ALD films should also produce negligible gas diffusion pathways.

In this paper, Al_2O_3 ALD was explored on polyethylene (PE), poly(methyl methacrylate) (PMMA), polystyrene (PS), polypropylene (PP), and poly(vinyl chloride) (PVC). All of these polymers were spin-coated onto the surface of a quartz crystal microbalance (QCM) sensor or a Si(100) wafer.[10] Spin-coating produces smooth polymer films with thicknesses between 0.1 and 0.5 μm. The Al_2O_3 ALD was then examined by either monitoring the mass changes on the polymer films using the QCM sensor or by measuring the deposited film thickness on the Si(100) wafers using a surface profilometer. Together with recent Fourier transform infrared (FTIR) measurements of Al_2O_3 ALD on low-density PE particles,[9] these QCM and surface profilometry measurements clarify Al_2O_3 ALD on polymers. These results lead to a model for Al_2O_3 ALD nucleation and growth on polymers.

II. Experimental Details

A. Al_2O_3 ALD in a Viscous Flow Reactor. The viscous flow ALD reactor design has been described in detail in previous publications.[18] The specific reactor for this research consisted of a multiport chamber with a 10 cm diameter glass viewport. Stainless steel tubes with an inside diameter of 1.4 in. led in and out of this chamber. Ultra-high-purity N_2 carrier gas flowed continuously through the stainless steel tubes at a mass flow rate of ~35 sccm. A mechanical pump obtained a pressure of ~300 mTorr inside the reactor with this N_2 carrier gas flow. Heating tape maintained the chamber reactor at a temperature of ~85 °C. The upstream end of the flow tube was fitted with two channels for the introduction of the chemical precursors into the N_2 carrier gas.

$Al(CH_3)_3$ [trimethylaluminum (TMA)] with a 97% purity was obtained from Aldrich. HPLC-grade H_2O was obtained from Optima. The TMA was held in a stainless steel vessel and connected to the reactor using stainless steel tubing. The H_2O was contained in a 25 mL glass bulb and attached to the stainless steel tubing leading to the reactor using an Ultratorr union. Both reactants were maintained at room temperature at ~20 °C. The TMA and H_2O precursors were alternatively introduced into the N_2 carrier gas using pneumatic switching valves.

The introduction of TMA and H_2O was adjusted using conductance needle valves to ensure a precursor pressure transient peak of ~100 mTorr. This pressure transient was measured by a 10 Torr Baratron attached to the flow tube between the precursor switching valves and the central chamber. In all the experiments with each of the polymers, the exposure pressures of TMA and H_2O were constant. A separate mechanical pump was attached through pneumatic switching valves to the upstream ends of the precursor lines.[18] This mechanical pump removed excess precursor after each reactant exposure.

The Al_2O_3 ALD film growth was accomplished by two self-limiting surface reactions that have been described in previous work:[4−6,19]

$$\text{(A) } Al{-}OH^* + Al(CH_3)_3 \rightarrow Al{-}O{-}Al(CH_3)_2{}^* + CH_4 \quad (1)$$

$$\text{(B) } Al{-}CH_3{}^* + H_2O \rightarrow Al{-}OH^* + CH_4 \quad (2)$$

where the asterisks denote the surface species. The Al_2O_3 ALD growth occurs during alternating exposures to TMA and H_2O. With repetition of the surface reactions given by eqs 1 and 2, Al_2O_3 growth occurs very linearly with the number of AB cycles. Typical measured Al_2O_3 ALD growth rates are 1.1−1.2 Å per AB cycle.[5,19] The Al_2O_3 ALD films are very smooth and extremely conformal to the underlying substrate.[2,5,7]

After each reactant exposure, there is a N_2 purging period to remove all nonreacted gases. Due to the thermally sensitive nature of the polymeric substrates, the Al_2O_3 ALD growth was performed at 85 °C. These low temperatures for Al_2O_3 ALD have been successfully demonstrated in prior work.[6] Because of these lower growth temperatures, the reactant purges are long and the reactant exposure sequence is 1-29-1-29. All of the times are given in seconds. This notation indicates a 1 s exposure to TMA, a 29 s purge of the excess TMA, a 1 s exposure of H_2O, and a 29 s purge of the excess H_2O.

The film growth was monitored with an in situ quartz crystal microbalance (QCM). The QCM was introduced through a 2.75 in. flange on the downstream side of the N_2 carrier stream. The QCM was positioned such that the QCM sensor head was in the center of the chamber. The QCM sensor head was also directly above the silicon substrates and visible through the glass viewport. QCM sensors were mounted in a Maxtek BSH-150 bakeable sensor head that was attached to a 2.75 in. conflated flange. The sensor head incorporated a tube for the flow of ~10 sccm of N_2 across the back surface of the QCM sensor to prevent thin film deposition.[18]

The QCM sensor measures the mass change during the Al_2O_3 ALD process. The sensor signal from the AT-cut quartz crystal at 6 MHz was measured with a Maxtek TM400 film thickness monitor. The resolution of the QCM measurements was 0.4 ng cm^{-2}. Assuming an Al_2O_3 density of 3.0 g cm^{-3}, this mass sensitivity translates into a resolution for the Al_2O_3 film thickness measurements of 0.013 Å. The Al_2O_3 ALD films were also grown on 25 mm square Si(100) substrates positioned in the central chamber on the bottom of the flow tube.

(14) Xu, Y.; Musgrave, C. B. *Chem. Mater.* **2004**, *16*, 646.
(15) Weaver, M. S.; Michalski, L. A.; Rajan, K.; Rothman, M. A.; Silvernail, J. A.; Brown, J. J.; Burrows, P. E.; Graff, G. L.; Gross, M. E.; Martin, P. M.; Hall, M.; Mast, E.; Bonham, C.; Bennett, W.; Zumhoff, M. *Appl. Phys. Lett.* **2002**, *81*, 2929.
(16) Graff, G. L.; Williford, R. E.; Burrows, P. E. *J. Appl. Phys.* **2004**, *96*, 1840.
(17) Groner, M. D.; Elam, J. W.; Fabreguette, F. H.; George, S. M. *Thin Solid Films* **2002**, *413*, 186.
(18) Elam, J. W.; Groner, M. D.; George, S. M. *Rev. Sci. Instrum.* **2002**, *73*, 2981.
(19) Ott, A. W.; McCarley, K. C.; Klaus, J. W.; Way, J. D.; George, S. M. *Appl. Surf. Sci.* **1996**, *107*, 128.

B. Polymer Film Preparation and Characterization. The experiments were conducted concurrently on thin polymer films spin-coated onto the QCM sensors and the Si(100) substrates. The unpolished QCM sensors were obtained from Maxtek. The polymer films were spin-coated onto the QCM crystal sensors or the silicon squares using a Laurell Technologies Model WS-400A-6NPP-Lite Single Wafer Spin Processor. For good film uniformity, solutions of 5 wt % polymer in solvent were utilized and spin-coated at 3000 rpm for 60 s.

All the polymers were prepared using solutions of 5 wt % polymer and spin-coated at 3000 rpm. These parameters were determined by testing solutions of all the polymers varying from 1 to 10 wt % polymer and 250−5000 rpm. Visual observation indicated that spin-coating at ≥3000 rpm yielded the smoothest films. Solutions of ≥5 wt % produced films that were thick enough to measure with surface profilometry and to remove easily from the Si(100) substrate using a razor blade. No further optimization was utilized to prepare the polymer films.

The polymer solids were obtained in powder, pellet, or rubbery solid form from Scientific Polymer Products Inc. The polymers used in this work were as follows: polyethylene (PE #536) MW = 1100 dissolved in decalin; poly(methyl methacrylate) (PMMA #424) MW = 15000 dissolved in acetone; polystyrene (PS #846) MW = 190000 dissolved in toluene; polypropylene atactic (PP #783) MW = 10000 dissolved in toluene; and poly(vinyl chloride) (PVC #645) MW = 90000 dissolved in cyclohexanone. Immediately prior to spin-coating, the polymer solutions were heated to ∼50 °C. The polyethylene solution required heating to ∼90−100 °C to dissolve fully the polymer by breaking up the clusters of solid polymer that are common at room temperature. The spin processor environment and all substrates were at room temperature during the spinning process.

After spin-coating the polymer films, the film thicknesses were measured with a Veeco Instruments Dektak 3 surface profilometer. To make the step measurement, a razor blade was used to remove a portion of the polymer from the silicon substrate and form a clean edge. High-temperature aluminum tape (3M #433) was also used to mask a part of the Si(100) surface that did not contain the polymer film. This Si(100) wafer with polymer, no polymer, and masked region with no polymer permits the measurement of the thickness of Al_2O_3 ALD film on both the Si(100) wafer and on the polymer spin-coated on the Si(100) wafer.

The prepared samples were placed in the reactor for a minimum of 1 h and a maximum of 24 h prior to Al_2O_3 ALD. This conditioning time allows the QCM to achieve a stable oscillation. This steady state occurs when the temperature of the QCM sensor is constant in the N_2 carrier gas stream. This stability is important for reliable QCM measurements.[20]

Surface profilometry measurements were performed after Al_2O_3 ALD on the patterned polymer films on the Si(100) substrates. The masking tape was removed from the Si(100) substrates with minimal epoxy residue. The remaining epoxy residue was subsequently cleaned easily with methanol. The profilometer was also equipped with an optical camera. This camera was used to analyze the polymer films and image the step region between the polymer film and the bare Si(100) substrate.

C. Quartz Crystal Microbalance Measurements of Polymer Films. The change in the oscillating frequency of the quartz crystal measures the increase of mass on the quartz crystal. The oscillation consists of the propagation of a shear wave at velocity $v_q = 334000$ cm s^{-1} in the quartz of density $\rho_q = 2.65$ g cm^{-3}. These two parameters give an acoustic impedance of $Z_q = \rho_q v_q = 8.85 \times 10^5$ g s^{-1} cm^{-2}.[21] A relationship between the initial quartz crystal frequency, f_q, the measured frequency with the deposited film, f_d, and the mass increase, m_d, is given by the Sauerbrey equation:[21,22]

$$m_d = (f_q - f_d)/C_f \qquad \text{where } C_f = 2f_q^{\,2}/(\rho_q v_q) \tag{3}$$

The linear Sauerbrey equation can measure accurate mass changes to within 1−2% for mass increases up to approximately 10−25 μg/cm^2 for the AT-cut quartz crystals.[21] This accuracy occurs for films of materials that are rigid and for low mass loadings of films with different acoustic impedances.[21]

Films with significant thickness or different acoustic impedance can dissipate the energy of the shear wave propagation. This energy dissipation will result in inaccuracies in the measurement of the mass sorption. The acoustic impedance of the polymer films is not known. However, a more general equation than the Sauerbrey equation can be written that accounts for different acoustic impedances.[21,23] This equation indicates that the mass measured by the QCM should be accurate to within 2% when $M < 0.1$ where $M = m_d/m_q$. In this range, films with widely different acoustic impedances yield the same functional dependence for M versus F where $F = (f_q - f_d)/f_q$. The mass of the quartz oscillator is $m_q \sim 0.1$ g cm^{-2}. The mass of the deposited polymer film is estimated to be $m_d \sim 1 \times 10^{-5}$ cm $\times$ 1 g cm^{-3} = 10 μg cm^{-2}. Based on these values, $M \sim 10$ μg cm^{-2}/0.1 g cm^{-2} = 1×10^{-4}. For this small M value ≪0.1, the QCM is operating in a linear range and the QCM measurements for Al_2O_3 ALD on the polymer should be very accurate.

In addition to the possible error introduced by the acoustic impedance of the polymer film, thermal instability can also introduce mass uncertainty.[20] The thermal drift was a maximum of ±1.0 °C in 60 min. For AT-cut quartz crystal resonators at 85 °C, the temperature fluctuation of $\Delta T = \pm 1.0$ °C may induce a frequency shift of $\Delta f = \pm 6$ Hz. This frequency shift is equivalent to $\Delta m = \pm 106$ ng cm^{-2}. Over the course of 60 min or 60 AB cycles, this temperature-induced effective mass change would be equivalent to 1.8 ng cm^{-2} per AB cycle. This effective mass change compares to the typical mass increase of ∼40 ng cm^{-2} per AB cycle during Al_2O_3 ALD. The ratio of 1.8:40 yields a possible mass error of ∼5%.

III. Results

A. Spin-Coated Polymer Films. The spin-coated polymer thin films exhibited different characteristics and surface roughnesses. Optical micrographs of these polymer films spin-coated onto Si(100) wafers are shown in Figure 1. The section of the polymer film that was removed using a razor blade is oriented on the right-hand side of all the optical micrographs.

The PVC−cyclohexanone solution presented no difficulties in spin-coating. The PVC film was the smoothest and most uniform film. As shown in Figure 1a, there are minimal crater or hill features in the PVC film. The surface roughness was on the order of 20 Å. The film appeared purple with small light blue streaks. The average thickness of the PVC film was 2400 ± 20 Å.

(20) Rocklein, M. N.; George, S. M. *Anal. Chem.* **2003**, *75*, 4975.
(21) Lu, C. Theory and Practice of the Quartz Crystal Microbalance. In *Applications of Piezoelectric Quartz Crystal Microbalances (Methods and Phenomena, Their Applications in Science and Technology)*; Lu, C., Ed.; Elsevier Science Ltd.: Amsterdam, 1984.
(22) Sauerbrey, G. Z. *Z. Phys.* **1959**, *155*, 206.
(23) Lu, C.; Lewis, O. *J. Appl. Phys.* **1972**, *43*, 4385.

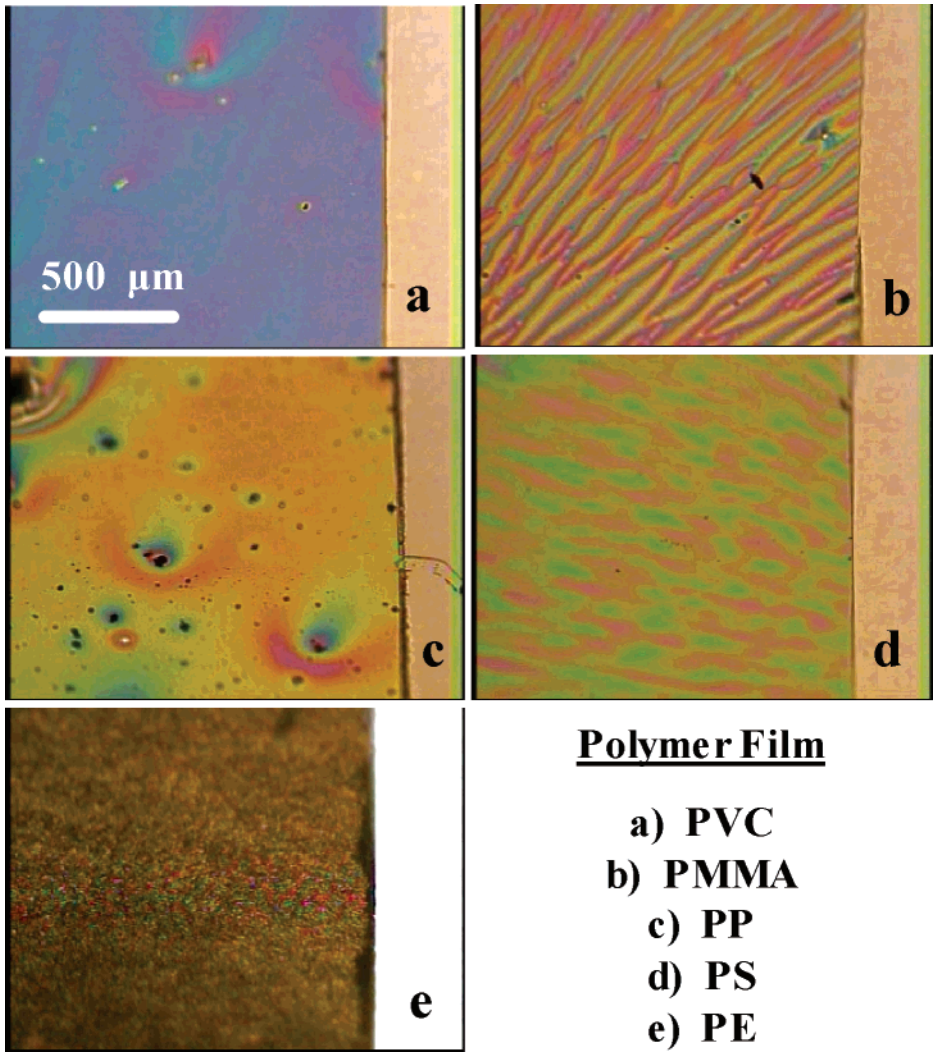

Figure 1. Optical micrographs of polymer films spin-coated onto Si(100) wafers. Polymer films are as follows: (a) PVC; (b) PMMA; (c) PP; (d) PS; and (e) PE.

The PMMA film revealed a regular repeating pattern of hills and valleys as displayed in Figure 1b. These hills and valleys were approximately 1000 Å high and radiated outward from the sample center. These features are an artifact of the spin-coating process. These undulations also gave the film a spectrum of colors from violet to red. The average thickness of the PMMA film was 4000 ± 1000 Å.

The PP film revealed no apparent striations but was marked by numerous particles and craters in the surface. A picture of the PP film is shown in Figure 1c. The overall color of the film was orange-yellow with the entire spectrum of colors visible around the defects. The average thickness of the PP film was 2000 ± 500 Å. The PS film exhibited a more radially striated pattern with definite hills and valleys observed visually as an alternating red and green pattern. The PS film is displayed in Figure 1d. The average thickness of the PS film was 3500 ± 100 Å.

The PE−decalin solution system proved difficult to manipulate effectively in the spin-coating process. These difficulties were attributed to the large temperature difference between the heated solution and the spin-coating environment. These conditions caused the film to condense unevenly across the silicon or QCM surface. Although the film was able to cover the entire surface, Figure 1e shows that the film is marked by craters and hill and valley features. These undulations have an approximate root-mean-square (RMS) roughness of ∼2500 Å. The appearance of the film was gray and grainy. The average thickness of the PE spin-coated film measured by profilometry was 3500 ± 2500 Å.

B. QCM Monitoring of Al_2O_3 ALD. The various polymers displayed different nucleation and growth behavior during Al_2O_3 ALD. The differences were greatest in the nucleation region. After the nucleation of the Al_2O_3 ALD film, Al_2O_3 growth rates were very linear. However, the exact Al_2O_3 mass deposition per AB cycle in the linear growth region varied between the various polymer films. These differences will be shown to reflect the different surface roughnesses of the polymer films.

1. Polystyrene. Figure 2 shows the QCM mass change in ng cm^{-2} versus number of AB cycles during Al_2O_3 ALD on polystyrene (PS) at 85 °C for 500 cycles. The number of AB cycles is also equivalent to time where each AB cycle corresponds to 60 s for the 1-29-1-29 exposure sequence. After a short nucleation period, the mass change is very linear versus number of AB cycles. The mass change averaged over eight separate experiments was 44 ± 16 ng cm^{-2} per AB cycle in this linear growth region. After the Al_2O_3 ALD

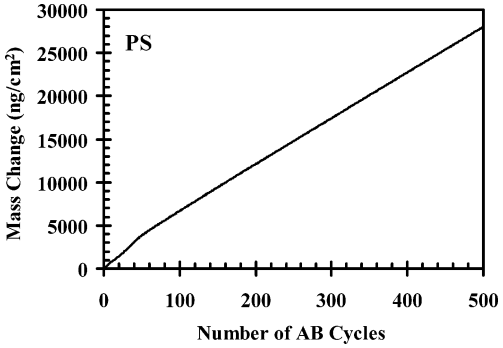

Figure 2. Mass change measured by QCM versus number of AB cycles during Al_2O_3 ALD on PS at 85 °C for 500 AB cycles. Each AB cycle is 60 s corresponding to 1-29-1-29 exposure sequence.

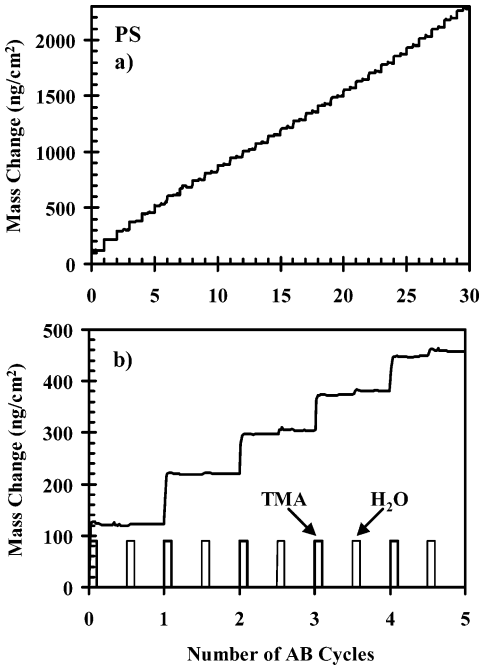

Figure 3. (a) Mass change at higher mass resolution measured by QCM versus number of AB cycles during Al_2O_3 ALD on PS at 85 °C for 30 AB cycles. (b) Mass change at highest mass resolution versus number of AB cycles during Al_2O_3 ALD on PS at 85 °C for 5 AB cycles. TMA and H_2O exposure sequence coinciding with mass changes is given for comparison.

growth ends at 500 AB cycles, there is no additional mass change.

Figure 3a shows the results for Al_2O_3 ALD on PS at 85 °C at higher mass resolution during the first 30 AB cycles. A total mass change of ~2300 ng cm^{-2} is observed after the 30 AB cycles. The Al_2O_3 ALD growth is not strictly linear over these first 30 AB cycles. The mass deposited during each AB cycle decreases slightly after the first 10−15 AB cycles. The structure of the mass changes versus TMA and H_2O exposures reveals distinct steps that are characteristic of Al_2O_3 ALD.[18] In addition, the mass change transients during the TMA and H_2O exposures also evolve during the first 10−15 AB cycles.

Figure 3b shows the mass changes at even higher mass resolution for the first 5 AB cycles. A large mass change of ~120 ng cm^{-2} is observed during the first TMA exposure on PS at 85 °C. The TMA and H_2O exposure sequence coinciding with the mass changes is also given for comparison. The TMA exposure occurs at whole-integer number of AB cycles. The H_2O exposure occurs at the half-integer

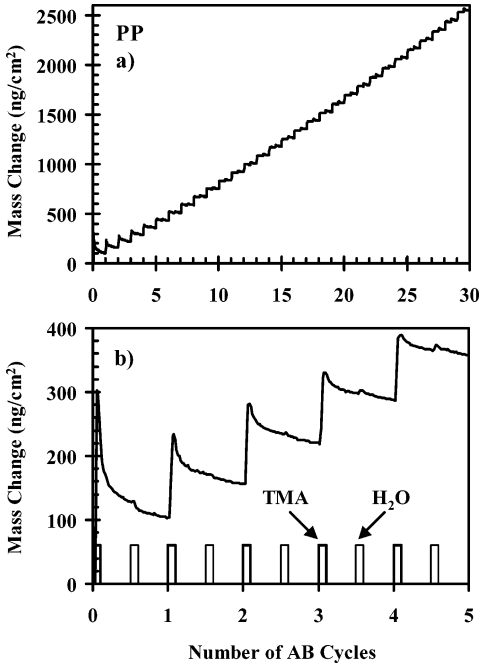

Figure 4. (a) Mass change measured by QCM versus number of AB cycles during Al_2O_3 ALD on PP at 85 °C for 30 AB cycles. (b) Mass change at higher mass resolution versus number of AB cycles during Al_2O_3 ALD on PP at 85 °C for 5 AB cycles. TMA and H_2O exposure sequence coinciding with mass changes is given for comparison.

number of AB cycles. The mass change of ~120 ng cm^{-2} is directly correlated with the TMA exposure. This TMA has either adsorbed on the PS polymer film or absorbed into the bulk of the PS polymer film. Only a small fraction of the adsorbed or absorbed TMA desorbs after the TMA exposure. The H_2O exposure stabilizes the mass change after the TMA exposure.

2. Polypropylene. Figure 4a shows the mass change in ng cm^{-2} versus number of AB cycles during Al_2O_3 ALD on polypropylene (PP) at 85 °C for 30 AB cycles. Large mass transients are observed during the TMA exposures in the nucleation region. After the nucleation period, Al_2O_3 ALD displays linear growth on PP with an average growth rate of 55 ± 22 ng cm^{-2} per AB cycle. A total mass change of ~2500 ng cm^{-2} is observed in Figure 4a after the 30 AB cycles. This total mass change is comparable to the ~2300 ng cm^{-2} observed in Figure 3a after 30 AB cycles of Al_2O_3 ALD on PS.

The first 5 AB cycles during Al_2O_3 ALD on PP at 85 °C are shown at higher mass resolution in Figure 4b. The TMA and H_2O exposure sequence coinciding with the mass changes is also displayed for comparison. The mass increase measured during the first TMA exposure is extremely large. A mass increase of ~300 ng cm^{-2} is observed prior to a mass decrease following the TMA exposure. This mass transient is consistent with the adsorption of TMA on PP and the absorption of TMA into PP followed by the desorption of some of the TMA.

The mass change during the second TMA exposure at the AB cycle number 1 in Figure 4b is also very large and >100 ng cm^{-2}. This mass transient decreases after the TMA exposure. This behavior is consistent with the adsorption or absorption of TMA followed by some TMA desorption. The

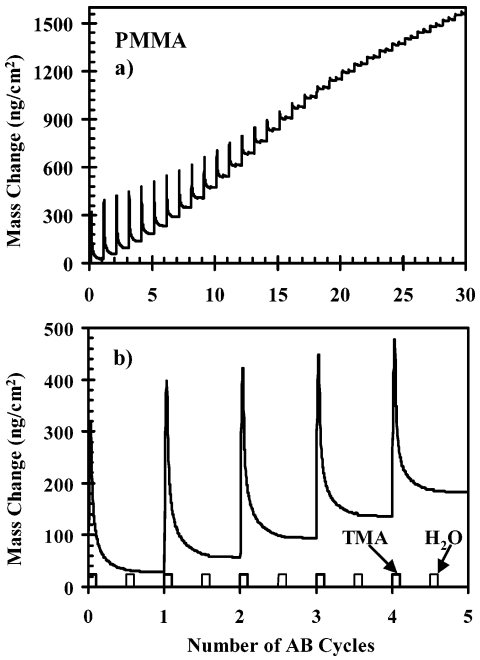

Figure 5. (a) Mass change measured by QCM versus number of AB cycles during Al_2O_3 ALD on PMMA at 85 °C for 30 AB cycles. (b) Mass change at higher mass resolution versus number of AB cycles during Al_2O_3 ALD on PMMA at 85 °C for 5 AB cycles.

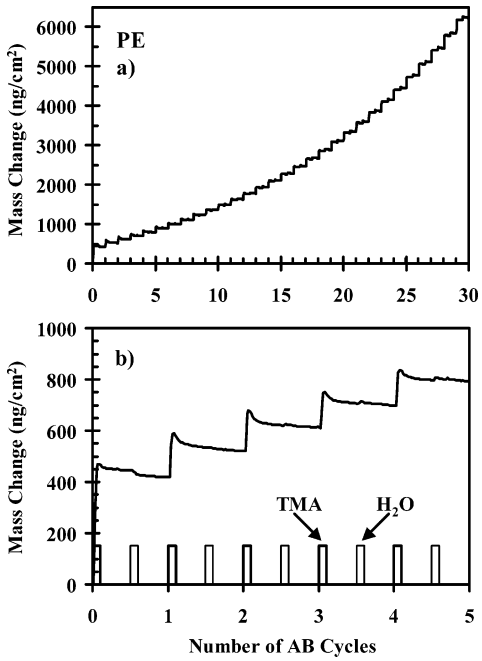

Figure 6. (a) Mass change measured by QCM versus number of AB cycles during Al_2O_3 ALD on PE at 85 °C for 30 AB cycles. (b) Mass change at higher mass resolution versus number of AB cycles during Al_2O_3 ALD on PE at 85 °C for 5 AB cycles.

third, fourth, and fifth TMA exposures also show large mass gains during the TMA exposures followed by mass decreases after the TMA exposure. However, the mass increases and decreases are smaller with increasing number of AB cycles.

3. Poly(methyl methacrylate). The absorption of large quantities of TMA during TMA exposures are also observed for Al_2O_3 ALD on poly(methyl methacrylate) (PMMA). Figure 5a shows the mass change versus number of AB cycles during Al_2O_3 ALD on PMMA at 85 °C. The QCM measures a rapid mass increase of ~300 ng cm^{-2} with the first exposure of TMA. The pronounced absorption of TMA during TMA exposures and desorption of TMA after the TMA exposures is dramatically evident during the first 10−15 AB cycles. Approximately 90% of the absorbed TMA mass is lost after the TMA exposure. The nucleation period for Al_2O_3 ALD occurs during the first 20 AB cycles. During this nucleation period, TMA uptake gradually decreases with increasing number of AB cycles. Subsequently, a linear Al_2O_3 ALD growth rate is reached with an average growth rate of 49 ±10 ng cm^{-2} per AB cycle based on six separate experiments.

The first 5 AB cycles of Al_2O_3 ALD on PMMA at 85 °C at higher mass resolution are shown together with the TMA and H_2O exposure sequence in Figure 5b. The pronounced uptake of TMA during TMA exposures and equally precipitous loss of TMA after the TMA exposures are vividly apparent. A steady mass increase occurs with every AB cycle. The mass change levels off with the H_2O exposure. The H_2O exposure may react with the remaining TMA in the PMMA film and stop the desorption of this TMA from the film.

4. Polyethylene. Al_2O_3 ALD on polyethylene (PE) at 85 °C is shown in Figure 6a for the first 30 AB cycles. Figure 6b displays the first 5 AB cycles at higher mass resolution. The QCM measures a large mass gain during the first TMA exposure of ~450 ng cm^{-2}. This large TMA absorption is followed by minimal TMA desorption. The mass change decreases to only ~400 ng cm^{-2}. The H_2O exposure appears to stop the desorption of any remaining TMA.

A comparison of Figure 6b for PE and Figure 5b for PMMA reveals the large capacity for PE to adsorb TMA. The large mass gain of ~450 ng cm^{-2} during the first TMA exposures on PE is larger than the mass gain of ~300 ng cm^{-2} during the first TMA exposures on PMMA. In addition, PE has a higher retention of TMA. Subsequent TMA exposures also lead to large TMA absorption and large mass changes every AB cycle. After 30 cycles, a total mass change of ~6200 ng cm^{-2} is observed for Al_2O_3 ALD on PE. In comparison, a total mass change of ~1500 ng cm^{-2} is monitored in Figure 5a for Al_2O_3 ALD on PMMA after 30 cycles.

5. Poly(vinyl chloride). Figure 7a shows the results for Al_2O_3 ALD on poly(vinyl chloride) (PVC) films at 85 °C during the first 30 AB cycles. The absolute mass change of ~1200 ng cm^{-2} after 30 AB cycles is much less than the mass change observed for Al_2O_3 ALD on PE after 30 cycles in Figure 6a. Figure 7b displays the first 5 AB cycles at higher mass resolution. Mass changes of only ~18−20 ng cm^{-2} are observed for the first several TMA exposures. Although the total TMA absorbed during the TMA exposures is much smaller for PVC compared with PP, PMMA, and PE, the absorbed TMA is not desorbed following the TMA exposures. The PVC retains the TMA and the measured mass change is nearly constant until the subsequent TMA exposure.

C. Surface Profilometry. Surface profilometry of the Si(100) wafer with polymer, no polymer, and masked region with no polymer allows the Al_2O_3 ALD thickness to be measured on both the Si(100) wafer and the polymer films

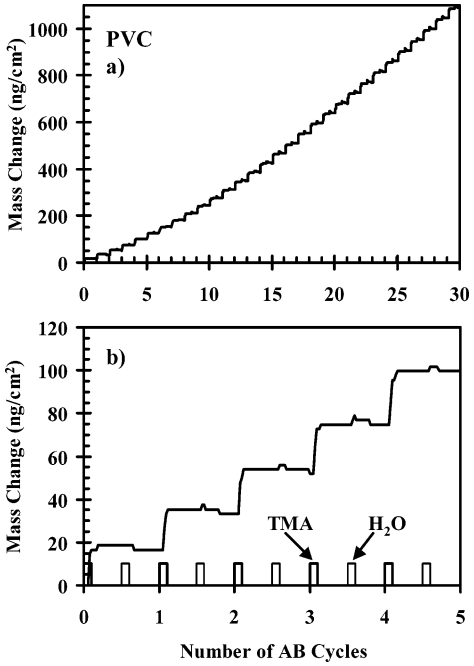

Figure 7. (a) Mass change measured by QCM versus number of AB cycles during Al_2O_3 ALD on PVC at 85 °C for 30 AB cycles. (b) Mass change at higher mass resolution versus number of AB cycles during Al_2O_3 ALD on PVC at 85 °C for 5 AB cycles.

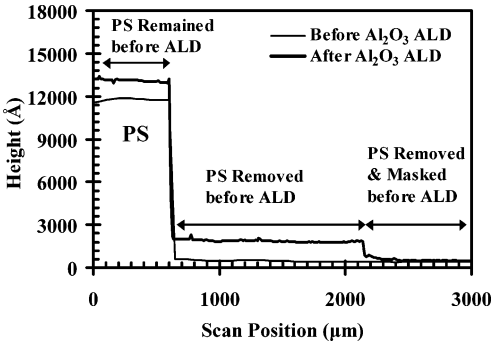

Figure 8. Surface profilometry scan on a patterned Si(100) wafer containing a PS polymer film before and after Al_2O_3 ALD at 85 °C. A mask was used to prevent Al_2O_3 ALD on a region of Si(100) wafer where PS polymer film was removed prior to Al_2O_3 ALD.

on Si(100). Figure 8 shows the results of a surface profilometry scan on a patterned Si(100) wafer containing a PS polymer film before and after Al_2O_3 ALD at 85 °C. The profile before Al_2O_3 ALD shows the PS polymer thickness on Si(100) obtained after removing a region of the PS film using a razor blade. The thickness of the PS film on the Si(100) wafer is ~11500 Å. The PS film is flat and very conformal to the Si(100) wafer. The profile after Al_2O_3 ALD shows that the Al_2O_3 ALD film thickness after 1000 AB cycles is conformal with a thickness of ~1250 Å on both the PS film and the Si(100) wafer.

Similar results were observed for the other polymers. However, most of the other polymer films were not as smooth as the PS film. Figure 9a shows the surface profilometry scan of a patterned Si(100) wafer containing a PMMA polymer film before and after Al_2O_3 ALD at 85 °C. The Al_2O_3 ALD conformally coated both the Si(100) wafer and the PMMA polymer film spin-coated to the Si(100) wafer. The distinct oscillations of the PMMA polymer film are observed both before and after Al_2O_3 ALD.

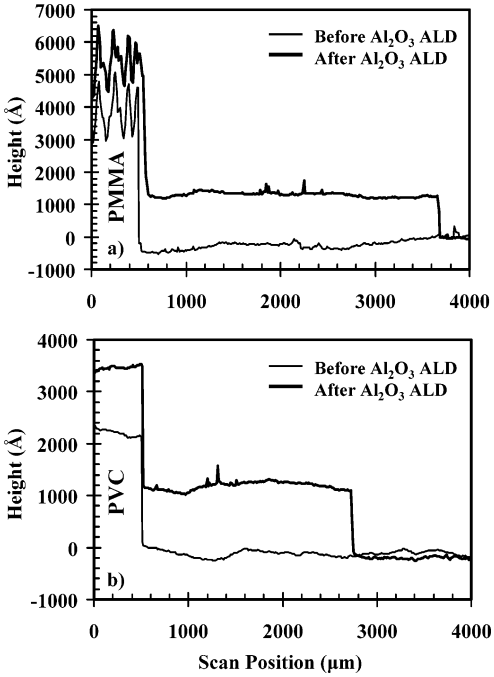

Figure 9. Surface profilometry scans on a patterned Si(100) wafer containing (a) PMMA and (b) PVC polymer films before and after Al_2O_3 ALD at 85 °C: Masks were used to prevent Al_2O_3 ALD on region of Si(100) wafer where polymer film was removed prior to Al_2O_3 ALD.

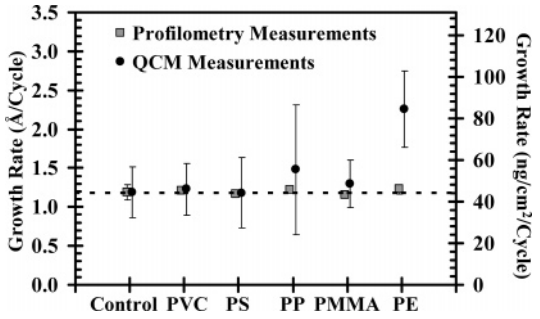

Figure 10. Al_2O_3 ALD growth rates measured on Si(100) wafers and various polymers. Gray squares show thickness growth rates determined by surface profilometer before and after 1000 AB cycles of Al_2O_3 ALD. Solid circles show mass growth rates measured by QCM. Mass growth rates are scaled to compare with thickness growth rates by assuming that 44.5 ng cm^{-2} per AB cycle on unpolished QCM sensor equals 1.2 Å per AB cycle.

The surface profilometry scan of the patterned Si(100) wafer containing a PVC film is displayed in Figure 9b. The PVC polymer film is very smooth before and after Al_2O_3 ALD. The Al_2O_3 ALD thickness of ~1250 Å after 1000 AB cycles is observed both on the Si(100) wafer and the PVC polymer on the Si(100) wafer. Similar surface profilometry results were observed for the PP polymer film. The only polymer that could not be evaluated using surface profilometry was the PE film. The surface roughness of the PE film was too large to obtain meaningful profilometry measurements before and after Al_2O_3 ALD.

Figure 10 displays a summary of the results for the Al_2O_3 ALD growth rate measured on the Si(100) wafers and the various polymers. These growth rates were determined using the surface profilometer to measure the step heights before and after 1000 AB cycles of Al_2O_3 ALD on both the Si(100) wafer and the polymer films spin-coated to the Si(100) wafer. These growth rates were the average of between

2 and 8 individual experiments for each polymer film under the same reaction conditions. The control experiment was a Si(100) wafer containing no polymer film.

Figure 10 shows that the Al_2O_3 ALD growth rate is consistently ~1.2 Å per AB cycle on the Si(100) wafers. A very similar Al_2O_3 ALD growth rate was also measured on the polymer films spin-coated to the Si(100) wafers. The Al_2O_3 ALD growth rates on the Si(100) wafers were very reproducible and the error bars are less than the size of the data points for some of the samples. These results are in good agreement with previous measurements of the Al_2O_3 ALD growth rate.

The mass growth rates measured by the QCM are also shown in Figure 10. The control experiment shows the Al_2O_3 mass growth rate measured directly on QCM sensors with no polymer film. These control experiments yield a growth rate of 44.5 ±11.4 ng cm^{-2} based on the results from eight separate experiments performed on several different QCM sensors. This growth rate is higher than the expected growth rate of 34.5 ng cm^{-2} on a flat surface at 85 °C[6] because the original QCM sensors were unpolished and have a higher surface area. These mass growth rates measured with the QCM are scaled to compare with the profilometry measurements by assuming that 44.5 ng cm^{-2} per AB cycle on the unpolished QCM sensors equals 1.2 Å per AB cycle. Additional surface roughness of the polymer film on the QCM sensor will lead to mass growth rates that are larger than 44.5 ng cm^{-2}. These Al_2O_3 ALD growth rates measured on the polymer films display much larger error bars because of the variability of the spin-coated polymer films.

IV. Discussion

The QCM and surface profilometry results demonstrate that Al_2O_3 ALD can be used to coat a variety of polymer films. The PS, PP, PMMA, PVC, and PE polymers were chosen based on their availability and widespread use. The QCM results for Al_2O_3 ALD on these various polymer films reveal similarities as well as differences. Most of the differences are observed in the Al_2O_3 ALD nucleation region. The similarities are observed in the Al_2O_3 ALD growth region after nucleation.

A. Mass Changes during Initial TMA Exposures. Distinct mass increases are observed during the initial TMA exposures on the various polymer films. These mass increases vary dramatically between the polymers. Small mass increases of ~20 ng cm^{-2} are measured during the initial TMA exposures on PVC. Intermediate mass increases of ~120 ng cm^{-2} are observed during the initial TMA exposures on PS. Large mass increases of 300, 320, and 460 ng cm^{-2} are measured during the initial TMA exposures on PP, PMMA, and PE, respectively. In addition, the stabilities of the TMA in the polymer films are very different. PS, PE, and PVC retain most of the TMA after the TMA exposures. PP and PMMA lose most of the TMA after the TMA exposures.

The magnitude of the mass increases during the initial TMA exposures can be calibrated in terms of monolayers of TMA. Liquid TMA has a density of 0.725 g cm^{-3} and a molar mass of 72.086 g mol^{-1}. The number density of liquid TMA obtained from this density and molar mass is $\rho = 6.05 \times 10^{21}$ cm^{-3}. Based on this liquid number density, one monolayer of TMA is approximated by $\rho^{2/3} = 3.32 \times 10^{14}$ cm^{-2}. Given a mass of 1.197×10^{-22} g for one TMA molecule, the mass of one monolayer of TMA is 39.7 ng cm^{-2}. This monolayer mass can be used to interpret the QCM mass increases. The mass increases may result from adsorption of TMA onto the polymer surface or absorption of TMA into the polymer bulk.

The small mass increases of ~20 ng cm^{-2} measured during the initial TMA exposures on PVC are less than one TMA monolayer. These mass increases can be interpreted as TMA adsorption onto the polymer surface or absorption into the near surface region of the polymer bulk. In contrast, the large mass increases of 300, 320, and 460 ng cm^{-2} measured during the initial TMA exposures on PP, PMMA, and PE, respectively, must be interpreted as both TMA adsorption onto the polymer surface and absorption into the polymer bulk. These mass increases are consistent with the absorption of between 7 and 12 TMA monolayers on the QCM sensor. Given that the original QCM sensor was unpolished and has a higher surface area than the geometric surface area, the mass increases represent TMA coverages of between 5 and 9 monolayers on or in the polymer films. These large mass increases suggest that TMA can easily permeate into the near surface region of the PP, PMMA, and PE polymer films.

The mass changes after the TMA exposures reveal different TMA retention abilities for the various polymers. Although the TMA uptake by PVC is small, the TMA is retained by PVC after the TMA exposures. TMA is also retained by PS after intermediate levels of TMA uptake by PS. Likewise, PE retains most of the TMA even though the TMA uptake by PE is very large. In contrast, PP and PMMA show large TMA uptake but lose most of the TMA after the TMA exposures. This diversity of behavior suggests that there are several parameters that control the amount of TMA uptake and the retention of the TMA by the polymers.

These differences in mass changes and retention ability can be understood in terms of the chemical solubility and free volume of the polymer films. Permeability, P, is controlled by solubility, S, and diffusion, D. Permeability is defined by $P = S \times D$.[16] The large TMA uptake is associated with a large diffusion rate for TMA into the polymer film. The large diffusion rate is believed to result from more highly porous polymer films with large free volume. The retention of the TMA is associated with the chemical solubility of TMA in the polymer film. The chemical solubility is linked with the hydrophobic or hydrophilic nature of the polymer film.

Based on this model, PVC is interpreted to have small TMA uptake because PVC does not have large porosity or free volume. The mass increases are consistent with the adsorption of submonolayer quantities of TMA. These submonolayer quantities are retained after the TMA exposures because the TMA is strongly adsorbed on the PVC film surface or has a high solubility in the near surface region of the PVC film. In contrast, PP, PMMA, and PE are interpreted to have large TMA uptake because they have a large porosity or free volume. PE has a high chemical solubility for TMA and retains the TMA. PMMA does not

retain as much TMA because PMMA has a lower chemical solubility for TMA.

Although these interpretations are speculative, they are consistent with some of the properties of the various polymers. For example, PE is extremely hydrophobic as a result of being composed of only carbon and hydrogen. This highly nonpolar polymer would be expected to have a high chemical solubility for the nonpolar TMA. TMA is reported to have a high solubility in benzene.[24] In contrast, PMMA is more polar because of its carbonyl and oxygen composition resulting from the methyl ester side chain in each monomer unit. This more polar polymer would be expected to have a lower chemical solubility for the nonpolar TMA. The lower chemical solubility for TMA in PP compared with PE is not understood at this time.

The porosity or free volume of the polymer films is more difficult to characterize. The free volume may be dependent on the spin-coating procedure. The free volume is also higher at the surface of polymer films. Simulations have shown that amorphous polyethylene films have much lower densities and higher diffusivities at their surfaces.[25] Molecular dynamics studies have observed lower densities and a "dynamic interfacial layer" on a free surface of glassy atactic polypropylene.[26] Noncrystalline polymers also have exhibited significant free volumes of up to 10% in the near surface region.[27] The dual presence of amorphous and crystalline regions also affects the rate of diffusion in polymers.[28] A higher diffusion rate has been demonstrated for the amorphous regions due to randomness of passages between polymer chains and the fact that crystalline regions are effective barriers to any diffusion as a result of strong interpolymer chain bonding.[29]

Despite the general understanding of free volume and diffusivity in polymers, the differences between the small TMA uptakes by PVC and very large TMA uptakes by PP, PMMA, and PE cannot be easily explained at this time. A more complete understanding of these results must wait for additional information. The suggested interpretations are intended to generate discussion and help the formulation of additional questions and experiments.

B. Al_2O_3 ALD Growth Rates after Nucleation. The Al_2O_3 ALD nucleation period occurs during the first 10−20 AB cycles. During this time, the differences in the TMA uptake and TMA retention for the various polymers give rise to a wide range of masses deposited by Al_2O_3 ALD. After 30 AB cycles, the masses deposited by Al_2O_3 ALD on the polymers are approximately 1200, 1600, 2300, 2500, and 6200 ng cm^{-2} for PVC, PMMA, PS, PP, and PE, respectively. In comparison, a mass deposition rate of ∼44.5 ng cm^{-2} per AB cycle is measured for Al_2O_3 ALD on an unpolished QCM sensor. This mass deposition rate would yield a total mass deposited by Al_2O_3 ALD of ∼1335 ng cm^{-2} after 30 AB cycles.

The differences in nucleation behavior on the various polymers yield Al_2O_3 mass deposition that is either slightly less than or greater than the Al_2O_3 mass deposition expected for typical Al_2O_3 ALD on an unpolished QCM sensor. However, after the nucleation period, the Al_2O_3 ALD occurs with very close to the expected Al_2O_3 ALD deposition rate on an unpolished QCM sensor. The Al_2O_3 ALD thicknesses measured by the surface profilometer after 1000 AB cycles are nearly equivalent. Figure 10 shows that the surface profilometer measures growth rates that are very consistent at 1.2 Å per AB cycle on the Si(100) wafers. Very similar growth rates are observed on the polymer films spin-coated to the Si(100) wafer. Most of the differences in the nucleation behavior during the first 10−20 AB cycles are small compared with the Al_2O_3 deposited by 1000 AB cycles.

Figure 10 also shows that the growth rates measured by the QCM are very similar or slightly higher than the growth rates measured by the surface profilometer. The growth rates measured by the QCM are determined by dividing the total mass of Al_2O_3 deposited during Al_2O_3 ALD after 1000 AB cycles by 1000. The mass growth rates are scaled to compare with the profilometry measurements. This scaling assumes that 44.5 ng cm^{-2} per AB cycle on the unpolished QCM sensor equals 1.2 Å per AB cycle. The slightly larger QCM growth rates can be attributed to two factors. First, for PMMA, PS, PP, and PE, there is more Al_2O_3 mass deposited during the nucleation period after 30 AB cycles than is expected for Al_2O_3 ALD on an unpolished QCM sensor. However, this extra mass is small compared to the total mass deposited after 1000 AB cycles.

Second, the polymer surfaces have varying degrees of roughness. The surface roughness will produce more surface area and larger mass deposition rates than expected for Al_2O_3 ALD on an unpolished QCM sensor. The surface roughnesses that affect the QCM measurements may not be clearly discernible by the surface profilometry measurements. The surface profilometery measures a step height that may average substantial surface roughness. The radius of the diamond styllus on the profilometer is 12.5 μm. Consequently, lateral roughness with dimensions <15−20 μm will not be easily resolved by the surface profilometer.

C. Model for Al_2O_3 ALD Nucleation and Growth on Polymers. The QCM results presented in this paper and the previous results for Al_2O_3 ALD on low-density PE particles studied using Fourier transform infrared (FTIR) spectroscopy[9] can be used to formulate a model for Al_2O_3 ALD nucleation and growth on polymers. The earlier FTIR studies of Al_2O_3 ALD on low-density PE revealed that additional absorbance from C−H stretching vibrations was observed following TMA exposures.[9] This absorbance indicated that TMA can diffuse into the low-density PE particles. This TMA can be retained by the PE particles and react with the subsequent H_2O exposure.

The FTIR spectra also observed new O−H stretching vibrations and the loss of the C−H stretching vibrations after the H_2O exposures.[9] The O−H stretching vibrations appeared concurrently with new infrared absorbance features in the region of the Al_2O_3 bulk vibrational modes between 400 and 1000 cm^{-1}.[9] These infrared features grew progressively

(24) Lasserre, S.; Derouault, J. *New J. Chem.* **1983**, *7*, 659.
(25) Doruker, P.; Mattice, W. L. *Macromolecules* **1999**, *32*, 194.
(26) Mansfield, K. F.; Theodorou, D. N. *Macromolecules* **1991**, *24*, 6283.
(27) Jain, T. S.; de Pablo, J. J. *Macromolecules* **2002**, *35*, 2167.
(28) Compan, V.; Lopez-Lidon, M.; Andrio, A.; Riande, E. *Macromolecules* **1998**, *31*, 6984.
(29) Pavel, D.; Shanks, R. *Polymer* **2003**, *44*, 6713.

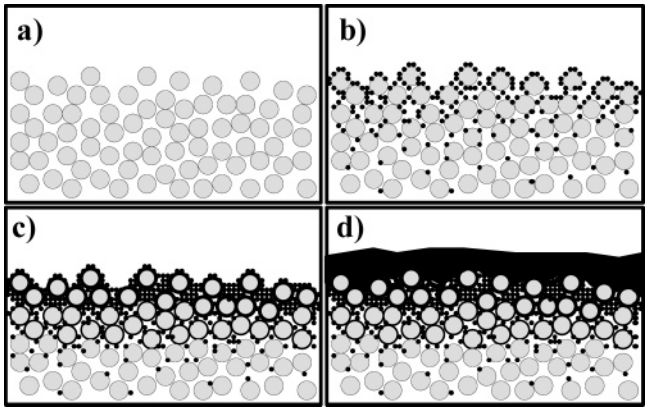

Figure 11. Model for Al_2O_3 ALD on polymer films showing (a) cross section of polymer film represented by loosely packed circles, (b) Al_2O_3 nucleation clusters forming from H_2O reaction with TMA trapped in the near surface region, (c) coalescence of Al_2O_3 clusters and closure of space between polymer chains, and (d) formation of dense Al_2O_3 film that grows on top of the polymer surface.

versus AB cycles on the low-density PE particles. After 40 AB cycles, the low-density PE particles were removed from the reaction chamber and analyzed using transmission electron microscopy (TEM). The TEM images displayed a conformal Al_2O_3 ALD film with a thickness that varied between 130 and 180 Å.[9]

The results of these previous FTIR investigations and the current QCM and profilometry experiments suggest that Al_2O_3 ALD involves the following steps: reactant diffusion, reactant retainment, Al_2O_3 cluster formation, and Al_2O_3 cluster coalescence to form a continuous Al_2O_3 film. In Figure 11, the polymer film is represented by loosely packed circles with a larger free volume in the near surface region. Since there are no initial hydroxyl groups within the polymer, the deposition proceeds because TMA molecules are trapped within the near surface region of the polymer film. Subsequent exposure to H_2O leads to reaction with TMA that forms Al_2O_3 nucleation clusters as shown in Figure 11b.

As these Al_2O_3 nucleation clusters in the near surface region grow during progressive TMA and H_2O exposures, they fill the space between the polymer chains. They eventually coalesce and close the space between the polymer chains. The Al_2O_3 ALD film becomes nearly continuous as shown in Figure 11c. Subsequent exposures lead to progressive Al_2O_3 ALD growth on the underlying polymer film as illustrated in Figure 11d. This continuous film should effectively block further H_2O and TMA reactant diffusion into the near surface region.

This model is consistent with the available FTIR, QCM, and surface profilometry results. By demonstrating Al_2O_3 ALD on the PS, PP, PMMA, PE, and PVC polymers using the QCM and surface profilometry studies, this model should be fairly general. Additional work in our laboratory for Al_2O_3 ALD on other polymers such as polyethylene naphthalene 2,6-dicarboxylate (PEN), Kapton, and polycarbonate (PC) also confirms the ubiquitousness of Al_2O_3 ALD on polymers.[11] The growth of Al_2O_3 ALD on these polymers supports the simple model.

Although Al_2O_3 ALD on polymers appears to be very general, questions remain about the effects of various polymer properties on Al_2O_3 ALD. The details of polymer film preparation, film history, and film annealing may all affect Al_2O_3 ALD because these factors can affect polymer free volume or crystallinity. Unfortunately, understanding all of these details was beyond the scope of this study. Additional experiments could be envisioned to explore these effects. While many of the polymer parameters remain to be examined, this investigation has illustrated the basic principles for Al_2O_3 ALD on polymers with these QCM measurements and a simple model. Hopefully, this investigation can serve as a springboard for more studies in the future.

V. Conclusions

This study explored the nucleation and growth during Al_2O_3 ALD on a variety of polymer films at 85 °C. The mass changes for polymers spin-coated onto QCM sensors revealed a range of behaviors consistent with the varying abilities of the polymers to adsorb, absorb, and retain the TMA reactant. The small mass increases during TMA exposures on PVC were consistent with submonolayer TMA adsorption or absorption. The large mass increases during TMA exposures on PP, PMMA, and PE were consistent with TMA absorption of between 5 and 9 TMA monolayers into the near surface region. Following the TMA exposures, the TMA is either retained or desorbs from the polymer. PS, PVC, and PE retained most of the adsorbed or absorbed TMA. In contrast, PP and PMMA lose a large fraction of the absorbed TMA after the TMA exposure.

The retained TMA reactant is available to react with the subsequent H_2O exposure. This reaction is believed to form small Al_2O_3 clusters in the near surface region of the polymer. With successive TMA and H_2O exposures, these Al_2O_3 clusters grow and eventually grow together and form a continuous Al_2O_3 film. The mass changes measured by the QCM reveal that the TMA diffusion into the polymers is impeded after 10−15 AB cycles. At this point, the Al_2O_3 ALD film is believed to form a diffusion barrier on the polymer. The growth of the Al_2O_3 ALD film is confirmed by surface profilometry measurements. Despite the very different nucleation behaviors on the various polymers, the total growth of Al_2O_3 ALD after 1000 AB cycles is very similar on both the uncoated Si(100) wafers and the polymer-coated Si(100) wafers.

The QCM and surface profilometry measurements reveal that Al_2O_3 ALD nucleates and grows readily on the various polymer substrates. This Al_2O_3 ALD growth occurs without specific chemical species that can react with TMA, such as hydroxyl (−OH) groups, on the surface or in the bulk of the polymer. The nucleation of Al_2O_3 ALD is facilitated by TMA diffusion into the polymers and the subsequent reaction of the retained TMA with H_2O. A model is developed for Al_2O_3 ALD on polymers that is consistent with the QCM measurements and recent Fourier transform infrared (FTIR) investigations of Al_2O_3 ALD on low-density PE particles. This model establishes an initial foundation to interpret ALD on polymers and will be developed further by future studies.

Acknowledgment. This work was funded by the National Science Foundation under Grant CHE-0408554 and the Air Force Office of Scientific Research.

CM050704D